Title

Long-term effects of wildfire smoke exposure during early life on the nasal epigenome in rhesus macaques

Authors

Brown, Anthony P

Cai, Lucy

Laufer, Benjamin I

et al.

Publication Date

2022

DOI

10.1016/j.envint.2021.106993

Peer reviewed

HHS Public Access

Author manuscript

Environ Int. Author manuscript; available in PMC 2022 February 17.

Published in final edited form as:

Environ Int. 2022 January ; 158: 106993. doi:10.1016/j.envint.2021.106993.

Long-term effects of wildfire smoke exposure during early life on the nasal epigenome in rhesus macaques

Anthony P. Brown[1], **Lucy Cai**[1], **Benjamin I. Laufer**[2], **Lisa A. Miller**[1,3], **Janine M. LaSalle**[2], **Hong Ji**[1,3,*]

[1]California National Primate Research Center, Davis, CA 95616, USA

[2]Department of Medical Microbiology and Immunology, MIND Institute, Genome Center, University of California, Davis, CA 95616, USA.

[3]Department of Anatomy, Physiology and Cell biology, School of Veterinary Medicine, University of California, Davis, CA 95616, USA

Abstract

Background—Wildfire smoke is responsible for around 20% of all particulate emissions in the U.S. and affects millions of people worldwide. Children are especially vulnerable, as ambient air pollution exposure during early childhood is associated with reduced lung function. Most studies, however, have focused on the short-term impacts of wildfire smoke exposures. We aimed to identify long-term baseline epigenetic changes associated with early-life exposure to wildfire smoke. We collected nasal epithelium samples for whole genome bisulfite sequencing (WGBS) from two groups of adult female rhesus macaques: one group born just before the 2008 California wildfire season and exposed to wildfire smoke during early-life (n = 8), and the other group born in 2009 with no wildfire smoke exposure during early-life (n = 14). RNA-sequencing was also performed on a subset of these samples.

Results—We identified 3370 differentially methylated regions (DMRs) (difference in methylation ≥ 5% empirical $p < 0.05$) and 1 differentially expressed gene (*FLOT2*) (FDR< 0.05, fold of change ≥ 1.2). The DMRs were annotated to genes significantly enriched for synaptogenesis signaling, protein kinase A signaling, and a variety of immune processes, and some DMRs significantly correlated with gene expression differences. DMRs were also significantly enriched within regions of bivalent chromatin (top odds ratio = 1.46, q-value < 3

[*]**Corresponding author**: Hong Ji, PhD, Department of Anatomy, Physiology and Cell Biology, School of Veterinary Medicine, California National Primate Research Center, University of California, Davis, CA, USA. Phone: 530-754-0679. hgji@ucdavis.edu.

Authors' contributions

HJ conceived the study in discussion with LAM and JML. APB drafted the manuscript with the help of HJ, BIL, JML and LAM. LC extracted DNA and RNA from nasal samples, prepared WGBS libraries. APB performed WGBS analysis with the help of BIL. APB performed other data analysis and visualization in discussion with HJ. All authors have approved the final version of this manuscript.

Competing interests

The authors declare they have no competing interests.

Ethics approval and consent to participate

Procedures in this study were approved by the UC Davis Institutional Animal Care and Use Committee.

Consent for publication

Not applicable.

Availability of data and materials

WGBS and RNA-seq data will be deposited to GEO upon manuscript acceptance.

× 10^{-6}) that often silence key developmental genes while keeping them poised for activation in pluripotent cells.

Conclusions—These data suggest that early-life exposure to wildfire smoke leads to long-term changes in the methylome over genes impacting the nervous and immune systems, but follow-up studies will be required to test whether these changes influence transcription following an immune/respiratory challenge.

Keywords

Wildfire smoke; whole genome bisulfite sequencing; RNA-sequencing; rhesus macaques; early life

BACKGROUND

According to the National Interagency Fire Center, there were 50,477 wildfires (4.7 million acres burned) in the United States in 2019. In total, 212 million Americans lived in counties affected by wildfires in 2011 (1). These wildfires have contributed to levels of air pollution in the United States that have been linked to premature death (2–5). About 20% of all fine particulate emissions in the U.S. are from wildfire smoke, while half of all particulate matter less than 2.5 μm in diameter ($PM_{2.5}$) in California resulted from wildfires (2). $PM_{2.5}$ are especially harmful, as these particles are able to penetrate the respiratory system and the lungs (2). Exposure to these particles has been associated with asthma, bronchitis, lung cancer, and cardiovascular disease (3–5). Young children are especially vulnerable to these negative health effects, as studies have linked air pollution exposure in children to reduced lung function (6, 7), reduced height-for-age (8), increased blood pressure (9), and an increased risk of developing asthma and eczema (10). Most of these studies, however, focused on the short-term effects of exposures to wildfire smoke or polluted air and none have performed an unbiased assessment of gene pathways impacted by wildfire smoke exposure.

A cohort of rhesus macaques (*Macaca mulatta*) that were exposed in their first three months of life to a harsh wildfire season in 2008 in California was previously studied to understand some of the long-term effects (macaques were 3–3.5 years of age when sampled in this prior study) of wildfire smoke exposure (11). Peripheral blood mononuclear cells (PBMCs) were cultured and challenged with either LPS or flagellin, and secretions of IL-8 and IL-6 were compared to macaques that were born in 2009 ($PM_{2.5}$ and ozone levels were much lower in 2009 compared to 2008) (11). Lung function was also compared between exposed and control macaques. Compared to control macaques, wildfire smoke-exposed macaques had significantly reduced lung volume. Female wildfire-exposed macaques showed reduced production of IL-8 compared to controls, while male wildfire-exposed macaques showed reduced production of IL-6 compared to controls (11). This study implied that early-life exposure led to a difference in IL-8 and IL-6 production following an immune challenge, but it was still unclear to what degree these macaques exhibited baseline differences at the level of epigenetics and gene expression.

Epigenetic changes (defined as modifications to DNA that do not alter the underlying sequence) such as DNA methylation have the potential to reflect past exposures with long-lived marks on genes. Current evidence specifically suggests that early-life exposures can lead to epigenetic reprogramming in the airways (12). The transcriptome, on the other hand, reflects current levels of gene expression in a sampled tissue. To test the hypothesis that early-life wildfire smoke exposure would result in detectable epigenetic differences to gene pathways reflecting cellular function, we performed the integrated unbiased approaches of whole genome bisulfite sequencing (methylome) and RNA-sequencing (transcriptome) from nasal epithelial samples collected the same cohorts of female macaques examined a decade earlier for lung functions and immune responses. Nasal epithelial tissue was sampled because they have been shown to be a biologically relevant proxy for airway epithelial cells in epigenomic studies of environmental exposures (13, 14). We identified a large number of genes associated with early-life exposure-related differential methylation involved in neuronal and immune signaling. In contrast, only one differentially expressed gene (*FLOT2*) was stably associated with early-life wildfire smoke exposure.

RESULTS

Exposure to wildfire smoke during infancy is associated with long-lasting changes to DNA methylation patterns in nasal epithelial cells.

To test the effects of early-life wildfire smoke-exposure on methylation status throughout the genome, we performed whole genome bisulfite sequencing on nasal epithelial samples collected from 22 adult rhesus macaques in 2019 (8 born in 2008 and exposed to high levels of $PM_{2.5}$ and ozone due to wildfires, 14 born in 2009 and therefore has relatively low levels of exposure to $PM_{2.5}$ and ozone; Figure 1, Table 1). Though there were several shared exposures to high levels of wildfire smoke $PM_{2.5}$ (> 35ug/m^3, the 24-hour $PM_{2.5}$ National Ambient Air Quality Standard) and ozone after the 2009 cohort was born (especially in the year of 2019), there was one high exposure event that only the 2008 cohort was exposed to in early-life (10 days above 35ug/m^3, Figure 1, Table 1). There were no significant, sustained wildfire events during the pregnancy periods for either group (Table 1). We assessed 26,609,677 CpG sites and identified 3370 differentially methylated regions (DMRs) between exposed and non-exposed samples (Figure 2, empirical $p < 0.05$, differences in methylation>5%). The majority of these DMRs were hypermethylated in exposed animals (2899, ~86%). A total of 114 (3.38%) of these DMRs were primarily located in CpG islands (15), 287 (8.52%) were located in CpG shores (0–2kb from island), 205 (6.08%) were located in CpG shelves (2–4kb from island), and 2764 (82.02%) were in the open sea (>4kb from island). This distribution was significantly different than expected by chance, with an enrichment towards CpG islands, shores, and shelves compared to regions assayed (Supplementary Figure 1). These 3370 DMRs were annotated to 2139 genes (Supplementary Table 1), of which 1852 genes were annotated to DMRs hypermethylated in the exposed group, while 376 genes were annotated to DMRs hypomethylated in the exposed group, and 89 genes were annotated to both hypermethylated and hypomethylated DMRs (examples of DMRs shown in Figure 3). The DMRs were significantly more associated with promoters and exons than expected by chance, while they were less associated with intergenic regions than expected by chance (Supplementary Figure 2). The

genes annotated to DMRs as a whole were significantly enriched (FDR < 0.05) for 186 IPA canonical pathways, including *axonal guidance signaling*, *synaptogenesis signaling pathway*, *protein kinase A signaling*, *IL-15 production*, *CXCR4 signaling*, and *Th1 and Th2 activation pathway* (Figure 4, Supplementary Table 2). Genes annotated to hypermethylated DMRs were enriched for 187 IPA pathways, 168 of which were also enriched in genes annotated to DMRs as a whole. The 19 unique IPA pathways enriched in hypermethylated DMRs include *14–3-3-mediated signaling, LPS-stimulated MAPK Signaling,* and *NF-κB activation by viruses* (Supplementary Table 3). Genes annotated to hypomethylated DMRs were enriched for 41 IPA pathways, 23 of which were also enriched in genes annotated to DMRs as a whole. The 18 unique IPA pathways enriched in hypomethylated DMRs include *dermatan sulfate biosynthesis, xenobiotic metabolism PXR signaling pathway*, and *HOTAIR regulatory pathway* (Supplementary Table 4).

Impact of wildfire smoke-associated DNA methylation changes on TF binding.

As the binding of transcription factors (TFs) are often influenced by DNA methylation, we performed a HOMER analysis to determine whether any transcription factor binding sites were enriched in these wildfire smoke-associated DMRs (16). A total of 131 transcription factor motifs were enriched in all DMRs ($q < 0.05$; Supplementary Table 5). Eight of the top ten most highly enriched TF motifs are part of the bZIP TF family (shown in Table 2). When testing for TF binding site enrichment in only DMRs that were hypermethylated in exposed macaques, six of the top ten were part of the bZIP TF family, while none of the top ten enriched TF binding sites in hypomethylated DMRs were part of the bZIP TF family (five out of ten contained homeobox motifs). Interestingly, the TFs whose binding sites were most enriched in all wildfire smoke-associated DMRs were primarily unmethylated (Table 2) in other ChIP-seq datasets (17), so the differential methylation could theoretically have a large impact on transcription factor binding and expression (18). In support of this, DNA methylation generally inhibits binding of bZIP TF members to DNA (18, 19).

Regions with hypomethylated DMRs are enriched for bivalent chromatin marks across tissue types.

In order to understand the gene regulatory role of regions with wildfire smoke-DMRs, we searched for the enrichment of 15 pre-defined chromatin states across 127 epigenomes from multiple tissues and cell types in the Roadmap Epigenomics project (20). After converting the *M. maculatta* coordinates into human (hg38) coordinates and using LOLA, the DMRs as a whole were enriched for bivalent chromatin marks (top odds ratio for any mark = 1.46, q-value $< 3 \times 10^{-6}$; Figure 5A). Bivalent chromatin marks represent co-existing activating and repressing marks, which often silence key developmental genes while keeping them poised for activation in pluripotent cells (21). Hypomethylated DMRs seemed to drive this enrichment (top odds ratio for any mark = 2.05, q-value < 0.02; Figure 5B), though hypermethylated DMRs showed enrichment (top odds ratio for any mark = 1.51, q-value $< 1 \times 10^{-6}$) for bivalent chromHMM (chromatin Hidden Markov Model) chromatin states as well (Figure 5C).

Correlation of DNA methylation and gene expression differences resulting from wildfire smoke exposure during infancy

To determine whether early-life exposure to wildfire smoke leads to detectable differences in gene expression later in life, we performed RNA-sequencing on 15 female rhesus macaques (6 born in 2008 and exposed to wildfire smoke, 9 born in 2009 and not directly exposed to the 2009 California wildfires). Out of the 2139 genes annotated to DMRs, 2128 had enough corresponding expression data to evaluate the correlation between expression and methylation. To identify genes where differential methylation may be ultimately leading to differential expression, we calculated the spearman rank correlation between methylation and expression levels for genes that were annotated to DMRs. In total, 172 genes were significantly correlated (spearman p-value < 0.05), with 76 genes showing a negative correlation and 96 showing a positive correlation between methylation and expression (Supplementary Table 9, two examples are shown in Figure 6). These 172 genes were enriched for 32 IPA pathway terms, including *leukocyte extravasation signaling, CCR5 signaling in macrophages,* and *MIF regulation of innate immunity* (Supplementary Table 10).

Early-life wildfire smoke exposure had a minimal effect on baseline genes expression levels.

A principal component analysis (PCA) and hierarchical clustering of all detected transcripts were performed to visualize how samples clustered based on expression (Supplementary Figure 3D). The top two principal components in a principal component analysis (PCA) explained 62% of the variation in the dataset. Exposed and non-exposed samples did not cluster separately in either the PCA or the hierarchical clustering analysis, implying no widespread transcriptomic difference between exposed and non-exposed individuals. After multiple hypothesis correction (FDR < 0.05, fold change ≥ 1.2; Supplementary Table 6), there was only one differentially expressed gene (*FLOT2*; Supplementary Table 6). None of the genes annotated to DMRs were significantly differentially expressed.

To identify co-expressed genes whose expression correlated with wildfire smoke-exposure status, we performed a weighted gene co-expression network analysis (WGCNA) (22). We identified 16 co-expressed modules using WGCNA. None of the modules were significantly associated with early-life exposure status ($p < 0.05$). The module that best correlated with exposure status was the purple module ($p = 0.1$; consisting of 585 genes, including *IFI44*, *IFNA21*, and *IL24*; Supplementary Figure 4, Supplementary Table 7). No genes in this module were significantly differentially expressed at an individual level, 19 genes were annotated to significant DMRs, and two genes had significantly correlated methylation and expression. The genes in this module were enriched (FDR < 0.05) for 21 IPA pathways, including *EIF2 signaling*, *mTOR signaling*, *Th17 activation pathway*, and *interferon signaling* (Supplementary Table 8).

DISCUSSION

Utilizing rhesus macaques that experienced the harsh conditions of the 2008 California wildfire season in their first three months, we have elucidated some of the long-term effects

of early-life exposure to wildfire smoke. Baseline methylation profiles generally clustered better by exposure status than expression profiles (Supplementary Figure 3). Many genes (2139) were annotated to differentially methylated regions between exposed and control macaques (empirical $p < 0.05$), while only 1 gene (*FLOT2*) was differentially expressed between these groups after multiple hypothesis correction (FDR < 0.05). Out of the genes annotated to differentially methylated regions, 172 had methylation levels that significantly correlated with expression levels across samples, indicating that the overall epigenetic regulatory landscape ultimately led to few significant differences in baseline expression. However, the changes in DNA methylation were significantly enriched at promoters and enhancers, and located at regions that transcription factors may bind, suggesting that they may have an impact on gene regulation.

FLOT2 (flotillin 2) encodes a caveolae-associated, integral membrane protein that belongs to the lipid raft family. Flotillins are implicated in variety of cellular functions, including regulation of G-protein coupled receptor signaling (23), endocytosis (24), cell-cell adhesion (25), uropod formation and migratory capacity of neutrophils and monocytes (26) and T cells (27). *FLOT2* also protected lung epithelial cells from Fas-signaling mediated apoptosis (28), and silica nanoparticles were found in Flotillin-1 and −2 marked vesicles in alveolar epithelial cell (29). However, its role in response to wildfire smoke exposure has not been reported.

One potential explanation for the few gene expression changes despite more widespread methylation differences is that many of these DMRs are in regions associated with bivalent chromatin marks. The differential methylation at these regions may not affect gene expression because the bivalent chromatin marks generally keep expression repressed, but poised for rapid activation during early development (30) or in cancer (31). This would imply that some of the methylation differences were due to early-life events that were not reflected in baseline transcript levels later in life. Additionally, although baseline gene expression was relatively similar between exposed and control macaques, one hypothesis is that the altered regulatory landscape could lead to differences in expression upon additional immune (or other) challenges. This hypothesis is supported by a previous study on macaques from these same cohorts that found differences in IL-6 (significant in males) and IL-8 (significant in females) production in peripheral blood mononuclear cells (PBMC) from wildfire smoke-exposed macaques compared to controls after a challenge with media, LPS, or flagellin (11). Out of 84 genes tested, only two (*RELB* and *REL*) showed significant differences in expression following a media challenge (essentially a comparison of baseline expression), while five genes were differentially expressed following a challenge with either LPS or flagellin (11). *RELB* was the only gene that was differentially expressed in all three tests, but the direction of change in challenged cells (increased *RELB* in cells from exposed animals) was opposite of what was found at baseline (decreased *RELB* in cells from exposed animals) (11). In summary, there were very few differences in baseline expression in the previous study between exposed and control cells, and even when there was differential expression, those patterns changed or became non-significant following an immune challenge. While the sample types (PBMCs vs. nasal epithelium) and ages of the macaques (adolescents vs. adults) differ between the prior study and the current study, they both support that early exposure to wildfire smoke did not lead to drastic differences

in baseline expression profiles between samples. Perhaps immediately following shared exposures to wildfire smoke, such as the one in 2018, there was more differential gene expression between the two cohorts, but gene expression returned to baseline levels and became indistinguishable by the time of sampling in 2019. Another potential explanation for differences in the degree of differential expression and differential methylation is that we had fewer samples for our differential expression analysis, potentially limiting our ability to identify differential expression compared to our ability to identify differential methylation. If there were widespread differences in expression due to exposure status, however, we expect that wildfire smoke-exposed samples would have clustered together in the principal component analysis and in hierarchical clustering analyses, so we postulate that this is not the major reason for the lack of differential expression.

Long-term effects of wildfire smoke exposure on the methylome

Our data implies that there are long-term effects on the methylome due to wildfire smoke exposures during infancy. DMRs were enriched for many pathways linked to asthma, COPD, or other pulmonary diseases, including *IL-15 production* (32, 33), *CXCR4 signaling* (34, 35), *Actin cytoskeleton signaling* (36, 37), *VDR/RXR activation* (38, 39), *Th1 and Th2 activation pathway* (40, 41), and *Wnt/β-catenin signaling* (42, 43) (Supplementary Table 2). Cytokines derived from T helper type 2 (Th2) cells have long been thought to play a critical role in allergic asthma through regulation of immunoglobulin E (IgE) synthesis (41, 44), but other T helper subsets (such as Th1) are starting to gain recognition for their role in asthma as well. Increased levels of the Th1 cytokine IFN- γ have been shown to exacerbate existing asthmatic responses (45) and increase airway hyperresponsiveness (44) in transgenic mice. *IFNGR2* (interferon gamma receptor 2) was differentially methylated in our comparison (as were several other Th1 related genes, including *IL6R*, *LOC694631/IFNA1/13-like*, and *NFATC1*), perhaps indicating that the early life wildfire smoke exposure has altered Th1 gene regulation, which could lead to differential responses to bacterial and viral infection. Additionally, hypermethylation of *IL6* and *IFNA13* was associated with idiopathic pulmonary fibrosis (IPF) (46), while hypermethylation of *IL6R* was associated with COPD in prior studies (47). *IL6R* and *IFNA13* were also hypermethylated in exposed macaques in our current study (Supplementary Table 11), indicating that changes in the Th1 pathway may contribute to the reduction in lung function noted in macaques exposed to wildfire smoke early in life (11). Th2-related genes that were differentially methylated in our dataset include *IL4R* and *TIMD4*, while there were several genes annotated to DMRs that were related to both the Th1 and Th2 pathways (including *CD4*, *IL10*, *IL12RB2*, *NFATC2*, *RUNX3*, and *SOCS3*). Hypermethylation of *NFATC2* (47), *RUNX3* (47), and *SOCS3* (48) has been associated with COPD (Supplementary Table 11). These three genes were also hypermethylated in wildfire smoke-exposed macaques versus controls.

Deletion of *Fra1*, the transcription factor with the most enriched motif in the DMRs (Table 2, Supplementary Table 5), in mice led to greater levels of progressive interstitial fibrosis (49). *Fra1* is a bZIP transcription factor and bZIP transcription factor binding is generally inhibited by methylation (18, 19). Meanwhile, overexpression of *Fra2* (another highly enriched bZIP TF motif in the DMRs) in mice lead to non-allergic asthma development (50). The other bZIP transcription factors whose motifs were among the top ten enriched

motifs have also all been linked to pulmonary disease (*ATF3* (51), *JunB* (52), *BATF* (53), and *AP-1* (49, 54)). The role of bZIP transcription factors in pulmonary disease pathogenesis combined with the sensitivity of bZIP to changes in methylation imply that the differences in methylation noted between wildfire smoke-exposed and non-exposed macaques could greatly impact how bZIP targets are regulated following a respiratory challenge. Overall, differences in methylation in Th1 and Th2-related genes (and the relation of those genes to asthma, IPF, and COPD pathogenesis; see Supplementary Table 11) may explain the long-term differences in lung function previously observed between wildfire smoke-exposed macaques and controls (11).

Interestingly, there is also recent research that suggests that exposure to air pollution can have negative neuropsychological effects in children (55, 56). The DMRs from our dataset were enriched in multiple IPA neurological pathways, including *axonal guidance signaling* (most significant pathway), *synaptogenesis signaling pathway* (third most significant pathway), and *neuropathic pain signaling in dorsal horn neurons* (Supplementary Table 2). Additionally, the top enriched biological process term in GOfuncR (57) was *neuron differentiation*, while the top enriched cellular component term was *synapse* (Supplementary Figure 5). Nasal epithelial tissue has also been considered to be a potential surrogate for neurons and neurodevelopment (58), our results showing enrichment for neuronal functions are consistent with this expectation. The effect of wildfire smoke on neurological development is understudied, but studies have shown that particles less than 0.1 μm in diameter (which are produced by wildfires) can cross the blood-brain barrier (59). Additionally, exposure to these ultrafine particles has been associated with ADHD, autism, and declines in school performance and memory in children (56). Along with this evidence from prior studies, the differential methylation of regions near genes involved in neurological pathways indicates that early-life wildfire smoke exposure could have a long-lasting impact on nervous system function.

Genes with correlated changes in methylation and expression are enriched for pathways associated with respiratory diseases

In addition to directly studying genes and enriched pathways associated with DMRs, we also wanted to identify genes that showed correlations between expression and methylation to get a better understanding of how differences in methylation modify mRNA expression. Though only one gene was differentially expressed between our groups following multiple hypothesis correction (*FLOT2*), there were many more genes annotated to DMRs that had a significant correlation between methylation and expression (172 in total; Supplementary Table 9). *MAPK10* (Spearman's $\rho \sim 0.75$) and *WNT8B* (Spearman's $\rho \sim 0.82$) were two other genes that were annotated to DMRs that showed a significant correlation between methylation and expression (Supplementary Table 9). Wnt signaling has been linked to *in utero* lung development and development/maturation during early life (alveologenesis) (60–62). Prior studies have shown that Wnt/β-catenin and the mitogen-activated protein kinase (MAPK) signaling pathway take part in the airway remodeling process in asthma (42). In a mouse model of asthma, blocking Wnt signaling reduced airway remodeling, while p38 MAPK expression was increased in asthmatic mice compared to controls (42). *MAPK10* expression was slightly higher on average in wildfire smoke-exposed macaques than

control macaques, and methylation was significantly positively correlated with expression (hypermethylated in exposed animals). WNT8B expression was slightly lower on average in exposed macaques, while methylation was significantly negatively correlated with methylation (hypomethylated in exposed animals). Neither of these genes were significantly differently expressed, however. Given the role of Wnt signaling and MAPK signaling in airway remodeling, it seems possible that changes in gene regulation could have contributed to the reduced lung function noted in wildfire smoke-exposed macaques (11).

Our study had several limitations. As previously touched upon, our current study included only female rhesus macaques, but a prior study with these macaques noted significant sex-specific differences in PBMCs challenged with LPS or flagellin. Male wildfire smoke-exposed macaques had significantly higher levels of IL-8 compared to controls, while female wildfire smoke-exposed macaques had significantly higher levels of IL-6 compared to controls (11). While IL-6 was not differentially expressed or methylated in our exposed macaques compared to controls, this does underscore that we may have missed some sex-specific differences in gene expression or methylation by sampling only female macaques for our current study. Indeed, studies have shown that there are sex-specific differences in expression between female and male asthmatics (63, 64), implying that the molecular underpinnings of asthma and other pulmonary issues may differ between the sexes. Additionally, our cohort of wildfire smoke-exposed macaques was roughly one year older than our cohort of control macaques. Studies have indicated that methylation patterns are associated with aging (epigenetic clocks) in humans (65, 66), so this is likely the case for rhesus macaques as well. Out of 2139 genes that were annotated to DMRs in our dataset, 20 were differentially methylated in a pattern that was consistent with the models from the previously referenced studies on epigenetic clocks. Based on these results, most of the differential methylation we observed cannot be explained by known differences in how methylation correlates with age. Another potential alternative explanation is that the differences in methylation we observed were due to greater cumulative exposure to pollutants in the older macaques. Table 1 shows that the difference in cumulative exposures to high levels of $PM_{2.5}$ and ozone between the two groups were roughly equivalent to the differences observed in the first three months of life, implying that these early exposures were key drivers of the noted differences between the groups. However, cumulative exposures below the current U.S. EPA standards were associated with increased mortality in a Medicare population (67), and they may also have an impact on the epigenome. The epigenetic effects of acute and chronic wildfire smoke exposure are worthy of further investigation. As previously discussed, we had a smaller sample size for our expression dataset (n = 13 after removing two outliers) than our methylation dataset (n = 22). This could explain why we saw fewer changes in expression overall, however samples appeared to cluster more closely based on exposure status for the methylation dataset than the expression dataset (Supplementary Figure 3). The p-values from DMRichR were empirical p-values calculated from permutation tests (68, 69). Although this puts our study at a higher risk of false-positive findings, these permutation p-values calculated by DMRichR were used to determine DMR significance in multiple published studies in combination with effect size (68–71). Given that our analysis of chromatin states relied on human hg38 annotations, we compared our macaque rheMac10 annotations to the hg38 annotations to make sure

they were similar enough. About 67% of the DMR gene annotations were exact matches after lifting over the coordinates to hg38. While 30% of DMRs had a different annotation, some of these differences were just due to differences in gene naming convention between the species. For example, one DMR was annotated to *LOC694631* (*IFNA1/13-like*) in rheMac10, while the lifted over DMR was annotated to *IFNA13* in hg38. In a broader pathway analysis, 90% of the IPA pathways enriched in DMRs using rheMac10 annotations were also enriched when we used hg38 annotations. We also focused our discussion on genes that were consistent between the two annotations.

One area of interest for future studies would be the stability of these changes. The exposure event took place in 2008, while samples were collected from the macaques in 2019. Over that relatively long course of time (the average lifespan for macaques in captivity is ~27 years (72)), the methylation profiles still clustered based on exposure status (Figure 2, Supplementary Figure 3). This implies that there are long-term impacts of wildfire smoke exposure on methylation, and that at least some of these changes are highly stable. An early study on DNA methylation stability involved sampling individuals three days apart to check for differences in DNA methylation. This study on 12 gene promoters indicated that methylation stability was marker dependent and varied based on sequence composition (73). Meanwhile, a large-scale study on how storage conditions affect methylation stability indicated that storing DNA samples in temperatures as high as four degrees Celsius for up to 20 years had no significant impact on methylation (74). Additionally, studies are needed to determine whether these epigenetic changes are associated with alterations in lung and immune functions, which will help to establish them as biomarkers for risk assessment in affected communities.

CONCLUSIONS:

In summary, our study revealed differences in methylation and gene expression in nasal epithelial samples between macaques that were exposed to wildfire smoke during early life and macaques that were not exposed to wildfire smoke during early life. The wildfire smoke associated DMRs were enriched for a variety of immune processes, but there were few significant expression differences at baseline between exposed and non-exposed macaques. Given the differences in methylation, perhaps differences in expression between these two groups would become apparent following an immune/respiratory challenge, but future studies would be required to explore this hypothesis. Our study indicates that wildfire smoke exposure in early life can have long-term impacts on the epigenome.

METHODS:

Animals

Wildfire smoke-exposed rhesus macaque monkeys born between April 1 and June 8, 2008 were housed in outdoor facilities at the CNPRC from birth to now (Table 1). Monkeys born between April 1 and June 8, 2009 were used as controls. $PM_{2.5}$ and ozone were measured by a California Air Resources Board air monitoring station (site no. 57,577) located 2.7 miles southeast of the California National Primate Research Center on the University of California Davis campus (Figure 1). Care and housing of animals complied with the provisions of

the Institute of Laboratory Animal Resources and conformed to practices established by the American Association for Accreditation of Laboratory Animal Care. Procedures in this study were approved by the UC Davis Institutional Animal Care and Use Committee.

Sample Collection and DNA/RNA Extraction

Nasal epithelium samples were collected from 22 female rhesus macaques (*Macaca mulatta*) housed at the California National Primate Research Center. Nasal cells have been shown in many studies to be a biologically relevant proxy for airway epithelial cells in epigenomic studies of lung diseases and effects of environmental exposures, particularly $PM_{2.5}$ exposures (13, 14, 75–79). Exposures of these animals to wildfire smoke were previously estimated (11). Eight of these macaques were born in 2008 and exposed to wildfire smoke from birth to 3 months old, while the other 14 were born in 2009 with low wildfire exposure from birth to 3 months old (Table 1, demographic comparison of two groups). We collected these nasal epithelium samples in 2019. RNA and DNA were isolated using the Allprep DNA and RNA kit (Qiagen) according to the manufacturer's instructions.

Library preparation for whole genome bisulfite sequencing (WGBS)

Whole genome bisulfite sequencing (WGBS) libraries were prepared for all 22 samples. Library quality was checked prior to sequencing using an Agilent 2100 Bioanalyzer system; library concentration was measured using a Qubit DNA high sensitivity assay. Each library was comprised of sample from a single individual; these individually barcoded libraries were then pooled and sequenced on two lanes from a NovaSeq 6000 S4 flow cell at PE150 using Swift's Accel-NGS Methyl-Seq Kit at the DNA Technologies and Expression Analysis Cores at the UC Davis Genome Center. We sequenced approximately 475 million paired end reads per sample that passed initial filters. Reads were demultiplexed using the bcl2fastq Illumina software.

WGBS read alignment, differential methylation analysis, pathway analysis, and chromatin state analysis

The CpG_Me pipeline (80–83) was utilized to align the WGBS data. Reads were trimmed using Trim Galore (82) to address methylation biases at the 5' and 3' end of reads (10 bases were trimmed from the 3' end of both read 1 and read 2, and 10 and 20 bases were trimmed from the 5' end of reads 1 and 2 respectively). The reads were aligned to the *M. mulatta* genome using Bismark (81), which was also used to deduplicate the aligned reads and generate CpG count matrices. Read quality and mapping quality were assessed using MultiQC (83). Differentially methylated regions between exposed and non-exposed macaques were identified using DMRichR (68, 84, 85), which uses the dmrseq (84) and bsseq (85) algorithms. Animal weight was adjusted for as a covariate. We used the default paramters for DMRichR, including requiring at least 1x coverage for all samples for a CpG, requiring a minimum of 5 CpGs for a DMR, performing 10 permutations for DMR and block analyses, and setting the single CpG coefficient required to discover testable background regions to be at least 0.05. Using DMRichR, candidate regions are identified based on differences in mean methylation between groups, then region-level metrics that account for mean methylation, CpG correlation, and coverage are computed. These region-level metrics are then compared to a pooled null distribution generated via permutations to

calculate an empirical p value for each candidate region (68, 69). Bsseq (85) was used to generate individual smoothed methylation values and heatmap visualizations. IPA (QIAGEN Inc., https://www.qiagenbioinformatics.com/products/ingenuitypathway-analysis) was used for pathway enrichment analysis. We also used GOfuncR (57) for GO enrichments based on DMR coordinates rather than gene names. HOMER (16) was used to identify enriched transcription factor binding motifs in the DMRs ($p < 0.05$), while we utilized MethMotif (17) to characterize methylation frequency of transcription factors whose binding motifs were enriched in the DMRs. We used the UCSC liftover tool (86) to lift DMR coordinates from rheMac10 to hg38 because chromatin state information was not available for *M. mulatta*. Locus Overlap Analysis (LOLA) (87) was used to determine whether DMRs were enriched for chromHMM (88) states relative to the background regions. The spearman correlation coefficient between gene expression and methylation levels for genes annotated to DMRs was used to determine whether significant methylation changes were associated with changes in gene expression ($p< 0.05$).

Library preparation for RNA-seq

RNAseq libraries were prepared for a total of 15 samples: 6 from wildfire smoke-exposed individuals and 9 from non-exposed individuals (Supplementary Table 12, comparison of these two groups). As some of the RNA samples were of low quantity, a special low-input RNA-seq pipeline were applied at the Genomics, Epigenomics and Sequencing Core of University of Cincinnati (89, 90). Briefly, polyA RNA was isolated using NEBNext Poly(A) mRNA Magnetic Isolation Module (New England BioLabs, Ipswich, MA) and enriched using SMARTer Apollo NGS library prep system (Takara Bio USA, Mountain View, CA). Libraries were prepared using NEBNext Ultra II Directional RNA Library Prep Kit (New England BioLabs), indexed, pooled and sequenced using Nextseq 550 sequencer (Illumina, San Diego, CA). Approximately 40 million reads passing filter per sample were generated under the sequencing setting of single read 1×85 bp. Reads were demultiplexed and adapters were trimmed using the bcl2fastq Illumina software.

RNA-seq read alignment, differential expression analysis, pathway analysis, and co-expression analysis

Read quality was checked using *FastQC* (91), then the reads were aligned to the *Macaca mulatta* genome (rheMac10, GenBank assembly accession: GCA_003339765.3) with *Bowtie2* (92). Transcripts were quantified using *RSEM* (93). The data from *RSEM* was congregated and converted into *DESeq2* (94) format using *tximport* (95). Sample clustering by expression (investigated via principal component analysis and hierarchical clustering) and detection of differentially expressed genes between wildfire smoke-exposed and non-exposed samples was done using *DESeq2* (94). Individual weight was included as a covariate in the differential expression analysis. Two samples (one wildfire smoke-exposed and one non-exposed sample) were excluded from all subsequent RNA-sequencing analyses because they were identified as outliers in the hierarchical clustering analysis (Supplementary Figure 6). The resulting log-fold change values were shrunken (following the recommendation from the *DESeq2* reference manual) using *apeglm* (96). Differentially expressed genes had FDR < 0.05 and an absolute shrunken fold change of at least 1.2. The Ingenuity Pathway Analysis (IPA) software (QIAGEN Inc., https://

www.qiagenbioinformatics.com/products/ingenuitypathway-analysis) was used for pathway analysis. Significantly enriched pathways in IPA had a p-value < 0.05.

Co-expressed modules of genes were found using WGCNA (22). The soft threshold (power) was set to 8 based on a plot of soft threshold vs scale free topology model fit. Modules that were too similar to one another (below a height of 0.5) were merged into one module. After merging, the final co-expression modules were tested for significant associations with wildfire smoke exposure and animal weight. Pathways enriched in genes in modules of interest were identified using IPA.

Supplementary Material

Refer to Web version on PubMed Central for supplementary material.

Acknowledgements

Nasal sampling was performed by staff members at CNPRC Research Services. The sequencing was carried out at the DNA Technologies and Expression Analysis Cores at the UC Davis Genome Center, supported by NIH Shared Instrumentation Grant 1S10OD010786-01.

Funding

This study was supported by a pilot grant from Environmental Health Sciences Center (NIEHS-P30ES023513) awarded to HJ. HJ was also supported by an Environmental Health Sciences Scholar Award (P30 ES006096), and NIH/NIAID R01AI141569-1A1. BL was supported Canadian Institutes of Health Research (CIHR) postdoctoral fellowship (MFE-146824) and a CIHR Banting postdoctoral fellowship (BPF-162684).

References

1. Knowlton K Where there's fire, there's smoke: wildfire smoke affects communities distant from deadly flames. 2013.
2. Dockery DW. Health effects of particulate air pollution. Ann Epidemiol. 2009;19(4):257–63. [PubMed: 19344865]
3. Brunekreef B, Holgate ST. Air pollution and health. Lancet. 2002;360(9341):1233–42. [PubMed: 12401268]
4. Li YJ, Takizawa H, Kawada T. Role of oxidative stresses induced by diesel exhaust particles in airway inflammation, allergy and asthma: their potential as a target of chemoprevention. Inflamm Allergy Drug Targets. 2010;9(4):300–5. [PubMed: 20887268]
5. Zhou Z, Liu Y, Duan F, Qin M, Wu F, Sheng W, et al. Transcriptomic Analyses of the Biological Effects of Airborne PM2.5 Exposure on Human Bronchial Epithelial Cells. PloS one. 2015;10(9):e0138267–e. [PubMed: 26382838]
6. Gehring U, Gruzieva O, Agius RM, Beelen R, Custovic A, Cyrys J, et al. Air pollution exposure and lung function in children: the ESCAPE project. Environ Health Perspect. 2013;121(11–12):1357–64. [PubMed: 24076757]
7. Urman R, McConnell R, Islam T, Avol EL, Lurmann FW, Vora H, et al. Associations of children's lung function with ambient air pollution: joint effects of regional and near-roadway pollutants. Thorax. 2014;69(6):540–7. [PubMed: 24253832]
8. Spears D, Dey S, Chowdhury S, Scovronick N, Vyas S, Apte J. The association of early-life exposure to ambient PM2.5 and later-childhood height-for-age in India: an observational study. Environmental Health. 2019;18(1):62. [PubMed: 31288809]
9. Rosa MJ, Hair GM, Just AC, Kloog I, Svensson K, Pizano-Zárate ML, et al. Identifying critical windows of prenatal particulate matter (PM(2.5)) exposure and early childhood blood pressure. Environ Res. 2020;182:109073. [PubMed: 31881529]

10. To T, Zhu J, Stieb D, Gray N, Fong I, Pinault L, et al. Early life exposure to air pollution and incidence of childhood asthma, allergic rhinitis and eczema. European Respiratory Journal. 2020;55(2):1900913.
11. Black C, Gerriets JE, Fontaine JH, Harper RW, Kenyon NJ, Tablin F, et al. Early Life Wildfire Smoke Exposure Is Associated with Immune Dysregulation and Lung Function Decrements in Adolescence. Am J Respir Cell Mol Biol. 2017;56(5):657–66. [PubMed: 28208028]
12. Gutierrez MJ, Perez GF, Gomez JL, Rodriguez-Martinez CE, Castro-Rodriguez JA, Nino G. Genes, environment, and developmental timing: New insights from translational approaches to understand early origins of respiratory diseases. Pediatr Pulmonol. 2021;56(10):3157–65. [PubMed: 34388306]
13. Somineni HK, Zhang X, Biagini Myers JM, Kovacic MB, Ulm A, Jurcak N, et al. Ten-eleven translocation 1 (TET1) methylation is associated with childhood asthma and traffic-related air pollution. The Journal of allergy and clinical immunology. 2016;137(3):797–805 e5. [PubMed: 26684294]
14. Sordillo JE, Cardenas A, Qi C, Rifas-Shiman SL, Coull B, Luttmann-Gibson H, et al. Residential PM2.5 exposure and the nasal methylome in children. Environ Int. 2021;153:106505. [PubMed: 33872926]
15. Jones PA. Functions of DNA methylation: islands, start sites, gene bodies and beyond. Nature reviews Genetics. 2012;13(7):484–92.
16. Heinz S, Benner C, Spann N, Bertolino E, Lin YC, Laslo P, et al. Simple combinations of lineage-determining transcription factors prime cis-regulatory elements required for macrophage and B cell identities. Mol Cell. 2010;38(4):576–89. [PubMed: 20513432]
17. Xuan Lin QX, Sian S, An O, Thieffry D, Jha S, Benoukraf T. MethMotif: an integrative cell specific database of transcription factor binding motifs coupled with DNA methylation profiles. Nucleic Acids Research. 2018;47(D1):D145–D54.
18. Yin Y, Morgunova E, Jolma A, Kaasinen E, Sahu B, Khund-Sayeed S, et al. Impact of cytosine methylation on DNA binding specificities of human transcription factors. Science. 2017;356(6337).
19. Héberlé É, Bardet AF. Sensitivity of transcription factors to DNA methylation. Essays in biochemistry. 2019;63(6):727–41. [PubMed: 31755929]
20. Ernst J, Kellis M. ChromHMM: automating chromatin-state discovery and characterization. Nature methods. 2012;9(3):215–6. [PubMed: 22373907]
21. Bernstein BE, Mikkelsen TS, Xie X, Kamal M, Huebert DJ, Cuff J, et al. A bivalent chromatin structure marks key developmental genes in embryonic stem cells. Cell. 2006;125(2):315–26. [PubMed: 16630819]
22. Langfelder P, Horvath S. WGCNA: an R package for weighted correlation network analysis. BMC Bioinformatics. 2008;9(1):559. [PubMed: 19114008]
23. Sugawara Y, Nishii H, Takahashi T, Yamauchi J, Mizuno N, Tago K, et al. The lipid raft proteins flotillins/reggies interact with Galphaq and are involved in Gq-mediated p38 mitogen-activated protein kinase activation through tyrosine kinase. Cell Signal. 2007;19(6):1301–8. [PubMed: 17307333]
24. Otto GP, Nichols BJ. The roles of flotillin microdomains--endocytosis and beyond. Journal of cell science. 2011;124(Pt 23):3933–40. [PubMed: 22194304]
25. Bodin S, Planchon D, Rios Morris E, Comunale F, Gauthier-Rouviere C. Flotillins in intercellular adhesion - from cellular physiology to human diseases. Journal of cell science. 2014;127(Pt 24):5139–47. [PubMed: 25413346]
26. Ludwig A, Otto GP, Riento K, Hams E, Fallon PG, Nichols BJ. Flotillin microdomains interact with the cortical cytoskeleton to control uropod formation and neutrophil recruitment. The Journal of cell biology. 2010;191(4):771–81. [PubMed: 21059848]
27. Giri B, Dixit VD, Ghosh MC, Collins GD, Khan IU, Madara K, et al. CXCL12-induced partitioning of flotillin-1 with lipid rafts plays a role in CXCR4 function. European journal of immunology. 2007;37(8):2104–16. [PubMed: 17634952]

28. Wei S, Moon HG, Zheng Y, Liang X, An CH, Jin Y. Flotillin-2 modulates fas signaling mediated apoptosis after hyperoxia in lung epithelial cells. PloS one. 2013;8(10):e77519. [PubMed: 24204853]
29. Kasper J, Hermanns MI, Bantz C, Utech S, Koshkina O, Maskos M, et al. Flotillin-involved uptake of silica nanoparticles and responses of an alveolar-capillary barrier in vitro. Eur J Pharm Biopharm. 2013;84(2):275–87. [PubMed: 23183446]
30. Mikkelsen TS, Ku M, Jaffe DB, Issac B, Lieberman E, Giannoukos G, et al. Genome-wide maps of chromatin state in pluripotent and lineage-committed cells. Nature. 2007;448(7153):553–60. [PubMed: 17603471]
31. Bernhart SH, Kretzmer H, Holdt LM, Juhling F, Ammerpohl O, Bergmann AK, et al. Changes of bivalent chromatin coincide with increased expression of developmental genes in cancer. Sci Rep. 2016;6:37393. [PubMed: 27876760]
32. Jonakowski M, Zioło J, Koćwin M, Przemęcka M, Mokros Ł, Panek M, et al. Role of IL-15 in the modulation of TGF-β1-mediated inflammation in asthma. Exp Ther Med. 2017;14(5):4533–40. [PubMed: 29104662]
33. Liu Z, Fan W, Chen J, Liang Z, Guan L. The role of Interleukin 15 in protein degradation in skeletal muscles in rats of chronic obstructive pulmonary disease. Int J Clin Exp Med. 2015;8(2):1976–84. [PubMed: 25932126]
34. Chen H, Xu X, Teng J, Cheng S, Bunjhoo H, Cao Y, et al. CXCR4 inhibitor attenuates allergen-induced lung inflammation by down-regulating MMP-9 and ERK1/2. Int J Clin Exp Pathol. 2015;8(6):6700–7. [PubMed: 26261552]
35. Henrot P, Prevel R, Berger P, Dupin I. Chemokines in COPD: From Implication to Therapeutic Use. International journal of molecular sciences. 2019;20(11):2785.
36. Tang DD, Gerlach BD. The roles and regulation of the actin cytoskeleton, intermediate filaments and microtubules in smooth muscle cell migration. Respiratory Research. 2017;18(1):54. [PubMed: 28390425]
37. D'Anna C, Cigna D, Di Sano C, Di Vincenzo S, Dino P, Ferraro M, et al. Exposure to cigarette smoke extract and lipopolysaccharide modifies cytoskeleton organization in bronchial epithelial cells. Experimental Lung Research. 2017;43(9–10):347–58. [PubMed: 29199880]
38. Iqbal SF, Freishtat RJ. Mechanism of action of vitamin D in the asthmatic lung. J Investig Med. 2011;59(8):1200–2.
39. Hu G, Dong T, Wang S, Jing H, Chen J. Vitamin D(3)-vitamin D receptor axis suppresses pulmonary emphysema by maintaining alveolar macrophage homeostasis and function. EBioMedicine. 2019;45:563–77. [PubMed: 31278070]
40. Martín-Orozco E, Norte-Muñoz M, Martínez-García J. Regulatory T Cells in Allergy and Asthma. Frontiers in Pediatrics. 2017;5(117).
41. Barnes PJ. Th2 cytokines and asthma: an introduction. Respiratory research. 2001;2(2):64–5. [PubMed: 11686866]
42. Jia X-X, Zhu T-T, Huang Y, Zeng X-X, Zhang H, Zhang W-X. Wnt/β-catenin signaling pathway regulates asthma airway remodeling by influencing the expression of c-Myc and cyclin D1 via the p38 MAPK-dependent pathway. Experimental and therapeutic medicine. 2019;18(5):3431–8. [PubMed: 31602218]
43. Guo L, Wang T, Wu Y, Yuan Z, Dong J, Li Xo, et al. WNT/β-catenin signaling regulates cigarette smoke-induced airway inflammation via the PPARδ/p38 pathway. Laboratory Investigation. 2016;96(2):218–29. [PubMed: 26322419]
44. Kim Y-M, Kim Y-S, Jeon SG, Kim Y-K. Immunopathogenesis of allergic asthma: more than the th2 hypothesis. Allergy Asthma Immunol Res. 2013;5(4):189–96.
45. Durrant DM, Metzger DW. Emerging roles of T helper subsets in the pathogenesis of asthma. Immunol Invest. 2010;39(4–5):526–49. [PubMed: 20450290]
46. Sanders YY, Ambalavanan N, Halloran B, Zhang X, Liu H, Crossman DK, et al. Altered DNA methylation profile in idiopathic pulmonary fibrosis. Am J Respir Crit Care Med. 2012;186(6):525–35. [PubMed: 22700861]

47. Morrow JD, Cho MH, Hersh CP, Pinto-Plata V, Celli B, Marchetti N, et al. DNA methylation profiling in human lung tissue identifies genes associated with COPD. Epigenetics. 2016;11(10):730–9. [PubMed: 27564456]
48. Vucic EA, Chari R, Thu KL, Wilson IM, Cotton AM, Kennett JY, et al. DNA methylation is globally disrupted and associated with expression changes in chronic obstructive pulmonary disease small airways. Am J Respir Cell Mol Biol. 2014;50(5):912–22. [PubMed: 24298892]
49. Rajasekaran S, Vaz M, Reddy SP. Fra-1/AP-1 Transcription Factor Negatively Regulates Pulmonary Fibrosis In Vivo. PLOS ONE. 2012;7(7):e41611. [PubMed: 22911824]
50. Gungl A, Biasin V, Wilhelm J, Olschewski A, Kwapiszewska G, Marsh LM. Fra2 Overexpression in Mice Leads to Non-allergic Asthma Development in an IL-13 Dependent Manner. Front Immunol. 2018;9(2018).
51. Gilchrist M, Henderson WR Jr., Clark AE, Simmons RM, Ye X, Smith KD, et al. Activating transcription factor 3 is a negative regulator of allergic pulmonary inflammation. J Exp Med. 2008;205(10):2349–57. [PubMed: 18794337]
52. Chen S, Yun F, Yao Y, Cao M, Zhang Y, Wang J, et al. USP38 critically promotes asthmatic pathogenesis by stabilizing JunB protein. Journal of Experimental Medicine. 2018;215(11):2850–67.
53. Übel C, Sopel N, Graser A, Hildner K, Reinhardt C, Zimmermann T, et al. The activating protein 1 transcription factor basic leucine zipper transcription factor, ATF-like (BATF), regulates lymphocyte- and mast cell-driven immune responses in the setting of allergic asthma. J Allergy Clin Immunol. 2014;133(1):198–206.e1–9. [PubMed: 24290279]
54. Caramori G, Casolari P, Adcock I. Role of transcription factors in the pathogenesis of asthma and COPD. Cell Commun Adhes. 2013;20(1–2):21–40. [PubMed: 23472830]
55. Suades-González E, Gascon M, Guxens M, Sunyer J. Air Pollution and Neuropsychological Development: A Review of the Latest Evidence. Endocrinology. 2015;156(10):3473–82. [PubMed: 26241071]
56. Holm SM, Miller MD, Balmes JR. Health effects of wildfire smoke in children and public health tools: a narrative review. Journal of Exposure Science & Environmental Epidemiology. 2020.
57. Grote S GOfuncR: Gene ontology enrichment using FUNC. R package version 1.10.0 ed2020.
58. Horiuchi Y, Kano S, Ishizuka K, Cascella NG, Ishii S, Talbot CC Jr., et al. Olfactory cells via nasal biopsy reflect the developing brain in gene expression profiles: utility and limitation of the surrogate tissues in research for brain disorders. Neurosci Res. 2013;77(4):247–50. [PubMed: 24120685]
59. Schraufnagel DE. The health effects of ultrafine particles. Exp Mol Med. 2020;52(3):311–7. [PubMed: 32203102]
60. Frank DB, Peng T, Zepp JA, Snitow M, Vincent TL, Penkala IJ, et al. Emergence of a Wave of Wnt Signaling that Regulates Lung Alveologenesis by Controlling Epithelial Self-Renewal and Differentiation. Cell Reports. 2016;17(9):2312–25. [PubMed: 27880906]
61. Hussain M, Xu C, Lu M, Wu X, Tang L, Wu X. Wnt/β-catenin signaling links embryonic lung development and asthmatic airway remodeling. Biochimica et Biophysica Acta (BBA) - Molecular Basis of Disease. 2017;1863(12):3226–42. [PubMed: 28866134]
62. De Langhe SP, Reynolds SD. Wnt signaling in lung organogenesis. Organogenesis. 2008;4(2):100–8. [PubMed: 19279721]
63. Gautam Y, Afanador Y, Abebe T, López JE, Mersha TB. Genome-wide analysis revealed sex-specific gene expression in asthmatics. Hum Mol Genet. 2019;28(15):2600–14. [PubMed: 31095684]
64. Mersha TB, Martin LJ, Biagini Myers JM, Kovacic MB, He H, Lindsey M, et al. Genomic architecture of asthma differs by sex. Genomics. 2015;106(1):15–22. [PubMed: 25817197]
65. Hannum G, Guinney J, Zhao L, Zhang L, Hughes G, Sadda S, et al. Genome-wide Methylation Profiles Reveal Quantitative Views of Human Aging Rates. Molecular Cell. 2013;49(2):359–67. [PubMed: 23177740]
66. Horvath S DNA methylation age of human tissues and cell types. Genome biology. 2013;14(10):R115. [PubMed: 24138928]

67. Shi L, Zanobetti A, Kloog I, Coull BA, Koutrakis P, Melly SJ, et al. Low-Concentration PM2.5 and Mortality: Estimating Acute and Chronic Effects in a Population-Based Study. Environ Health Perspect. 2016;124(1):46–52. [PubMed: 26038801]
68. Laufer BI, Hwang H, Vogel Ciernia A, Mordaunt CE, LaSalle JM. Whole genome bisulfite sequencing of Down syndrome brain reveals regional DNA hypermethylation and novel disorder insights. Epigenetics. 2019;14(7):672–84. [PubMed: 31010359]
69. Mordaunt CE, Jianu JM, Laufer BI, Zhu Y, Hwang H, Dunaway KW, et al. Cord blood DNA methylome in newborns later diagnosed with autism spectrum disorder reflects early dysregulation of neurodevelopmental and X-linked genes. Genome Med. 2020;12(1):88. [PubMed: 33054850]
70. Murat El Houdigui S, Adam-Guillermin C, Armant O. Ionising Radiation Induces Promoter DNA Hypomethylation and Perturbs Transcriptional Activity of Genes Involved in Morphogenesis during Gastrulation in Zebrafish. International Journal of Molecular Sciences. 2020;21(11):4014.
71. Laufer BI, Gomez JA, Jianu JM, LaSalle JM. Stable DNMT3L overexpression in SH-SY5Y neurons recreates a facet of the genome-wide Down syndrome DNA methylation signature. Epigenetics & Chromatin. 2021;14(1):13. [PubMed: 33750431]
72. Colman RJ, Anderson RM, Johnson SC, Kastman EK, Kosmatka KJ, Beasley TM, et al. Caloric restriction delays disease onset and mortality in rhesus monkeys. Science. 2009;325(5937):201–4. [PubMed: 19590001]
73. Byun H-M, Nordio F, Coull BA, Tarantini L, Hou L, Bonzini M, et al. Temporal Stability of Epigenetic Markers: Sequence Characteristics and Predictors of Short-Term DNA Methylation Variations. PLOS ONE. 2012;7(6):e39220. [PubMed: 22745719]
74. Li Y, Pan X, Roberts ML, Liu P, Kotchen TA, Jr AWC, et al. Stability of global methylation profiles of whole blood and extracted DNA under different storage durations and conditions. Epigenomics. 2018;10(6):797–811. [PubMed: 29683333]
75. Zhang X, Biagini Myers JM, Yadagiri VK, Ulm A, Chen X, Weirauch MT, et al. Nasal DNA methylation differentiates corticosteroid treatment response in pediatric asthma: A pilot study. PloS one. 2017;12(10):e0186150. [PubMed: 29028809]
76. Qi C, Jiang Y, Yang IV, Forno E, Wang T, Vonk JM, et al. Nasal DNA methylation profiling of asthma and rhinitis. The Journal of allergy and clinical immunology. 2020;145(6):1655–63. [PubMed: 31953105]
77. Yang IV, Pedersen BS, Liu AH, O'Connor GT, Pillai D, Kattan M, et al. The nasal methylome and childhood atopic asthma. The Journal of allergy and clinical immunology. 2016.
78. Cardenas A, Sordillo JE, Rifas-Shiman SL, Chung W, Liang L, Coull BA, et al. The nasal methylome as a biomarker of asthma and airway inflammation in children. Nat Commun. 2019;10(1):3095. [PubMed: 31300640]
79. Yang IV, Richards A, Davidson EJ, Stevens AD, Kolakowski CA, Martin RJ, et al. The Nasal Methylome: A Key to Understanding Allergic Asthma. American journal of respiratory and critical care medicine. 2017;195(6):829–31. [PubMed: 28294656]
80. Laufer BI, Hwang H, Jianu JM, Mordaunt CE, Korf IF, Hertz-Picciotto I, et al. Low-pass whole genome bisulfite sequencing of neonatal dried blood spots identifies a role for RUNX1 in Down syndrome DNA methylation profiles. Human Molecular Genetics. 2020;29(21):3465–76.
81. Krueger F, Andrews SR. Bismark: a flexible aligner and methylation caller for Bisulfite-Seq applications. Bioinformatics (Oxford, England). 2011;27(11):1571–2.
82. Martin M Cutadapt removes adapter sequences from high-throughput sequencing reads. 2011. 2011;17(1):3.
83. Ewels P, Magnusson M, Lundin S, Käller M. MultiQC: summarize analysis results for multiple tools and samples in a single report. Bioinformatics. 2016;32(19):3047–8. [PubMed: 27312411]
84. Korthauer K, Chakraborty S, Benjamini Y, Irizarry RA. Detection and accurate false discovery rate control of differentially methylated regions from whole genome bisulfite sequencing. Biostatistics. 2018;20(3):367–83.
85. Hansen KD, Langmead B, Irizarry RA. BSmooth: from whole genome bisulfite sequencing reads to differentially methylated regions. Genome Biology. 2012;13(10):R83. [PubMed: 23034175]
86. Kuhn RM, Haussler D, Kent WJ. The UCSC genome browser and associated tools. Brief Bioinform. 2013;14(2):144–61. [PubMed: 22908213]

87. Sheffield NC, Bock C. LOLA: enrichment analysis for genomic region sets and regulatory elements in R and Bioconductor. Bioinformatics. 2015;32(4):587–9. [PubMed: 26508757]

88. Ernst J, Kellis M. Chromatin-state discovery and genome annotation with ChromHMM. Nat Protoc. 2017;12(12):2478–92. [PubMed: 29120462]

89. Walsh KB, Zhang X, Zhu X, Wohleb E, Woo D, Lu L, et al. Intracerebral Hemorrhage Induces Inflammatory Gene Expression in Peripheral Blood: Global Transcriptional Profiling in Intracerebral Hemorrhage Patients. DNA Cell Biol. 2019;38(7):660–9. [PubMed: 31120332]

90. Rapp SJ, Dershem V, Zhang X, Schutte SC, Chariker ME. Varying Negative Pressure Wound Therapy Acute Effects on Human Split-Thickness Autografts. J Burn Care Res. 2020;41(1):104–12. [PubMed: 31420676]

91. Andrews S FastQC: A Quality Control Tool for High Throughput Sequence Data. 2010.

92. Langmead B, Salzberg SL. Fast gapped-read alignment with Bowtie 2. Nature Methods. 2012;9(4):357–9. [PubMed: 22388286]

93. Li B, Dewey CN. RSEM: accurate transcript quantification from RNA-Seq data with or without a reference genome. BMC Bioinformatics. 2011;12(1):323. [PubMed: 21816040]

94. Love MI, Huber W, Anders S. Moderated estimation of fold change and dispersion for RNA-seq data with DESeq2. Genome Biology. 2014;15(12):550. [PubMed: 25516281]

95. Soneson C, Love M, Robinson M. Differential analyses for RNA-seq: transcript-level estimates improve gene-level inferences [version 1; peer review: 2 approved]. F1000Research. 2015;4(1521).

96. Zhu A, Ibrahim JG, Love MI. Heavy-tailed prior distributions for sequence count data: removing the noise and preserving large differences. Bioinformatics. 2018;35(12):2084–92.

97. Kundaje A, Meuleman W, Ernst J, Bilenky M, Yen A, Heravi-Moussavi A, et al. Integrative analysis of 111 reference human epigenomes. Nature. 2015;518(7539):317–30. [PubMed: 25693563]

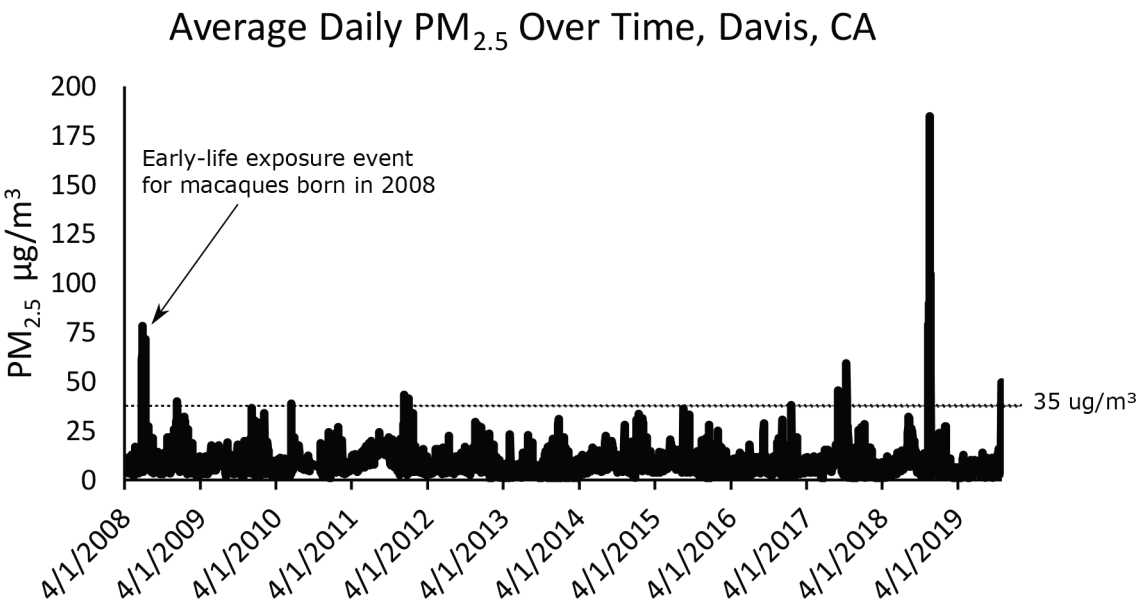

Figure 1:

Average daily $PM_{2.5}$ from April 2008 through October 2019 at the California Air Resources Board air monitoring station (site no. 57,577) located 2.7 miles southeast of the California National Primate Research Center on the University of California Davis campus. The dotted line at 35ug/m^3 represent the 24-hour $PM_{2.5}$ National Ambient Air Quality Standard. Note the arrow pointing to the early-life exposure event in macaques born in 2008. All other exposure events were shared between the two groups.

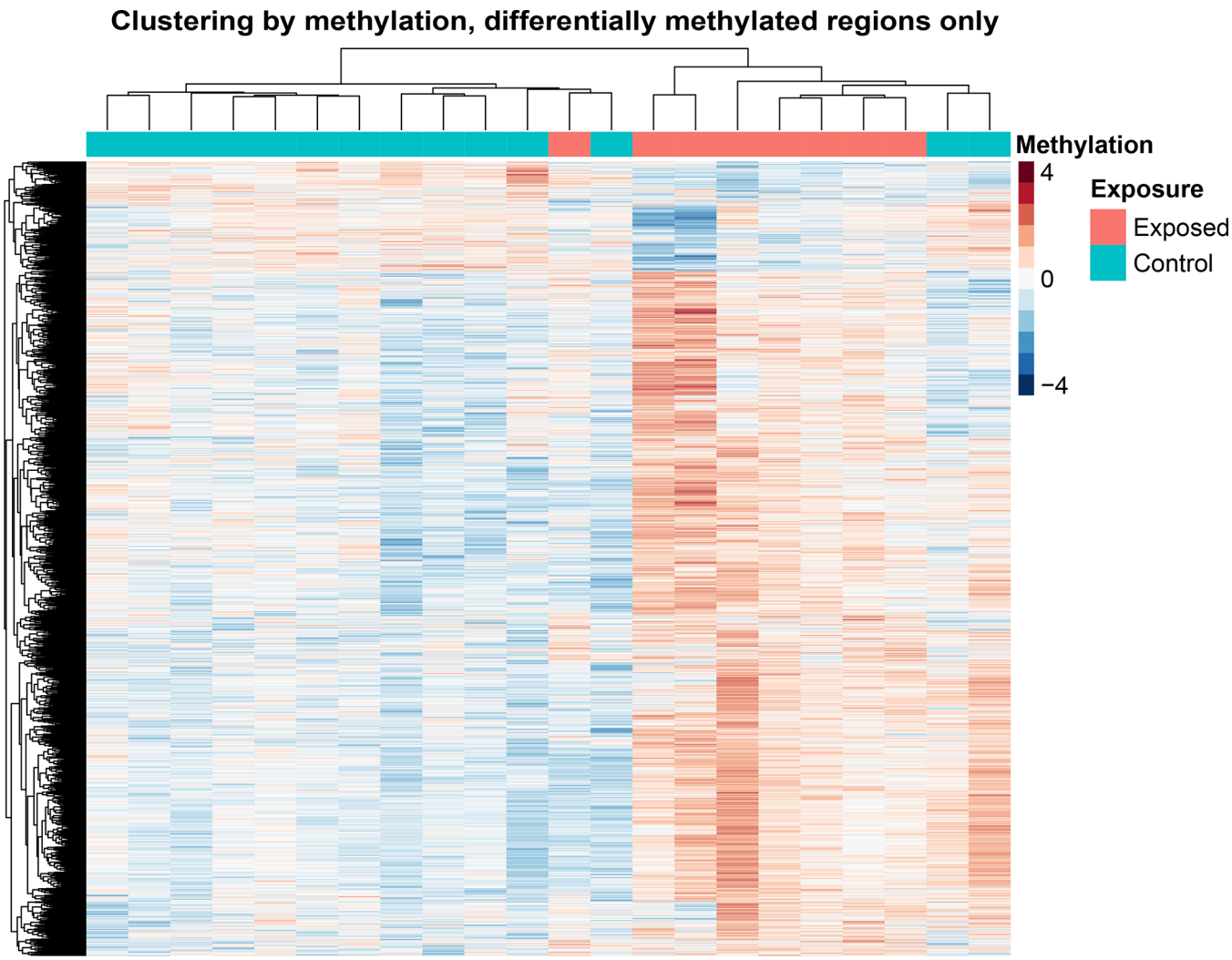

Figure 2:

Heatmap showing sample clustering based on methylation. The heatmap includes only differentially methylated regions (DMRs). The heatmap was normalized on a per row basis for visualization, therefore the values on the scales are relative rather than absolute.

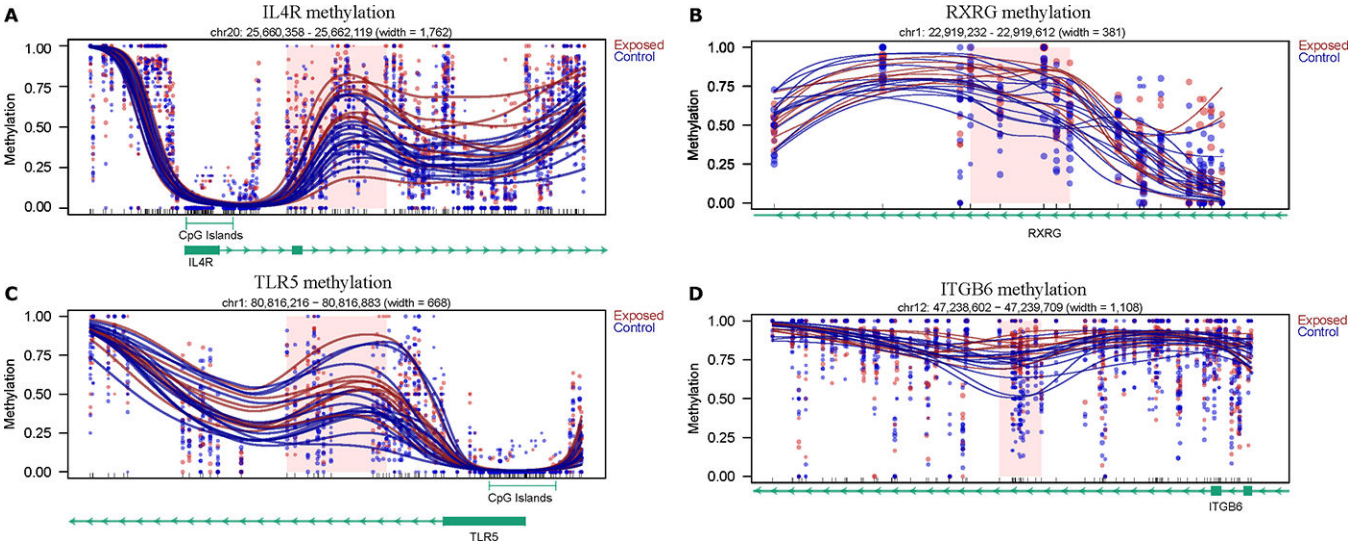

Figure 3:

Examples of differentially methylated regions (DMRs) between rhesus macaques exposed in the first three months of life to wildfire smoke and those that were not. A) *IL4R* (part of the STAT3 and Th2 canonical pathways). B) *RXRG* (part of the VDR/RXR Activation and the Aryl Hydrocarbon Receptor Signaling canonical pathways). C) *TLR5* (toll-like receptor that is part of the Phagosome Formation canonical pathway). D) *ITGB6* (part of the Paxillin Signaling and Integrin Signaling canonical pathways). Each dot represents the methylation percentage of one individual at one CpG site, while each line represents the smoothed average methylation level moving across the region. The red shaded boxes denote the specific DMR locations. Tracks for CpG islands (if present) or genes are included underneath each plot. For the gene tracks, a solid box indicates an exon, while the arrows indicate the direction of transcription.

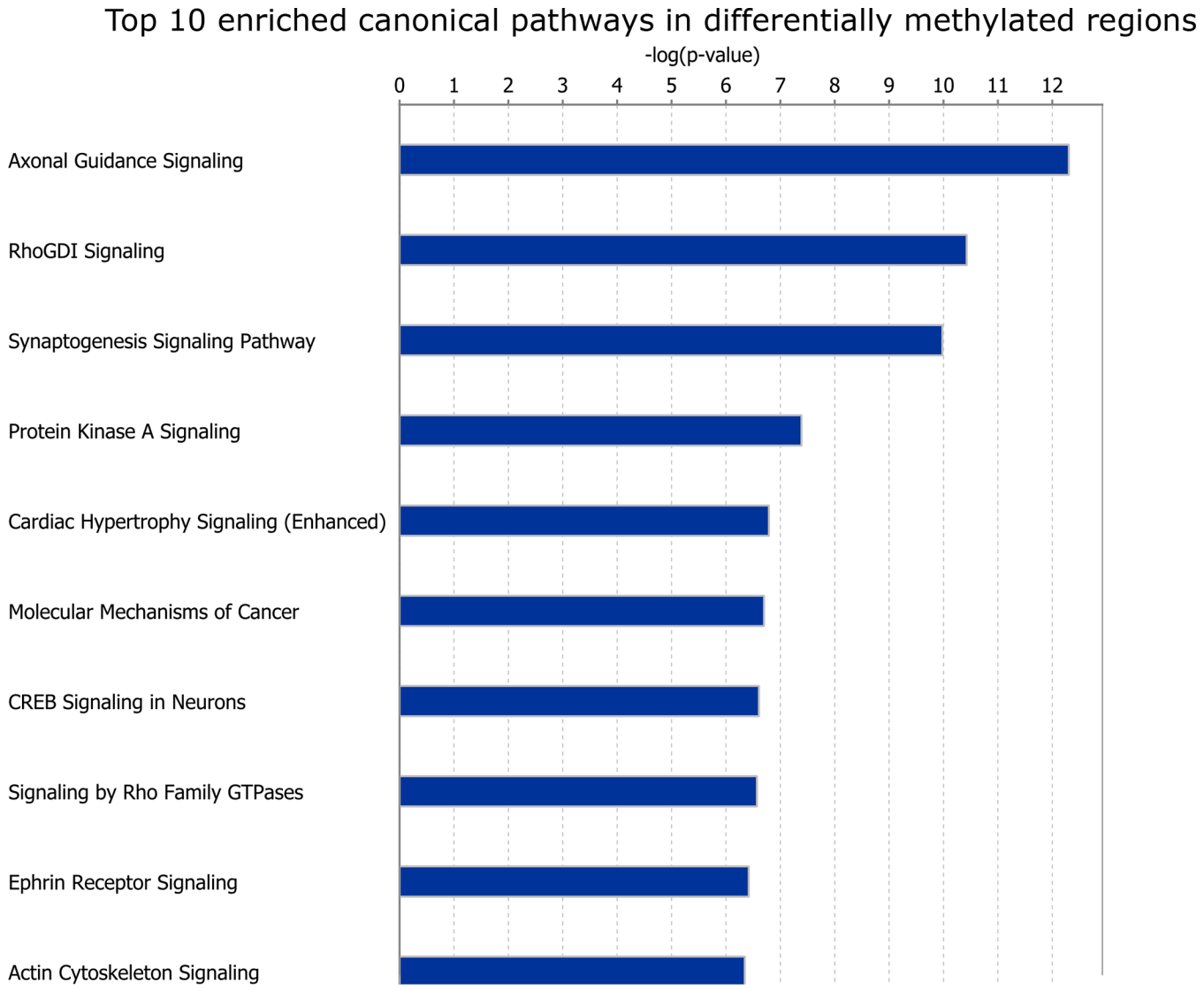

Figure 4:
Enriched pathway analyses for differentially methylated regions (DMRs). Only the top ten (out of 186) enriched Ingenuity Pathway Analysis (IPA) canonical pathways are shown.

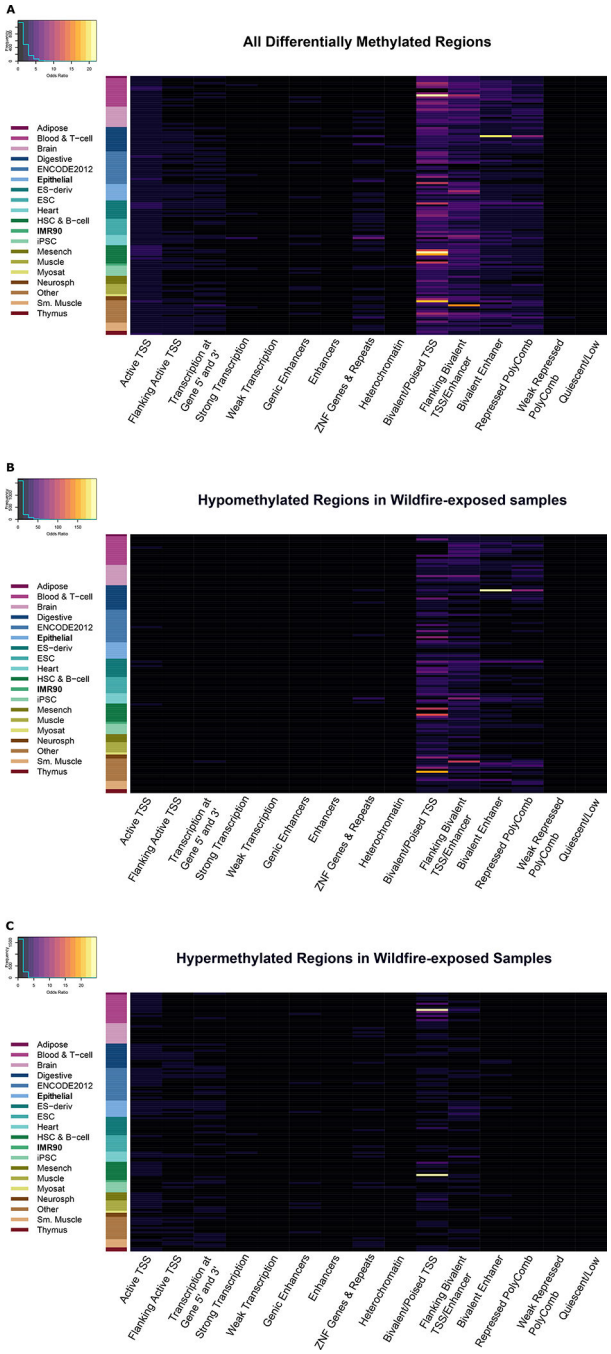

Figure 5:

Enrichment in chromHMM (88) states in A) all differentially methylated regions (DMRs), B) DMRs that were hypomethylated in wildfire smoke-exposed macaques, and C) DMRs that were hypermethylated in wildfire smoke-exposed macaques. The rows in the plot represent different datasets from different cell types from the NIH Roadmap Epigenomics Consortium (97). Epithelial and IMR90 are highlighted in the plots, as these are the closest to the nasal epithelial samples in our current study.

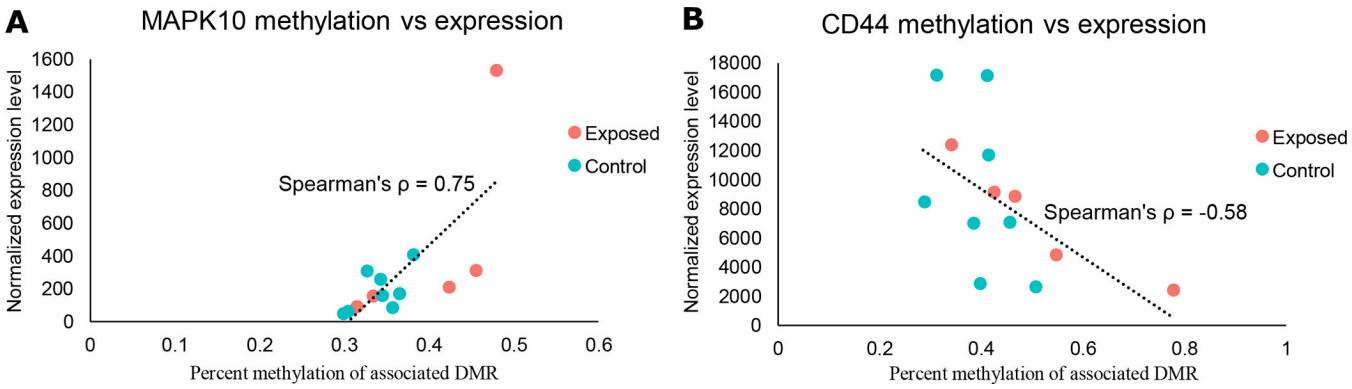

Figure 6.

Correlation plots between expression and methylation for A) *MAPK10* (part of the CXCR4 Signaling and the Leukocyte Extravasation Signaling canonical pathways) and B) *CD44* (part of the Leukocyte Extravasation Signaling and the Wnt/β-catenin Signaling canonical pathways). Each individual point represents one sample. Expression and methylation were significantly correlated (spearman p-value < 0.05) for both genes.

Table 1:

Demographic characteristics of animal populations

	2008 Birth Year	2009 Birth year	P
Participants			
N	8	14	
Age at sample collection (yr)	11.2±0.2	10.3±0.1	P<0.001
Weight at sample collection (kg)	8.61±1.60	10.11±2.78	0.12
Genetic background			
Indian	7	13	1.0
Mixed Indian-Chinese	1	1	
Corral diversity	8	13	1.0
Maternal Background			
Age at parturition (yr)	5.5±1.7	5.8±2.5	0.8
Genetic background			
Indian	7	12	1.0
Mixed Indian-Chinese	1	2	
Corral diversity	8	14	1.0
Ambient pollutant during pregnancy			
Days with $PM_{2.5}$ higher than 35ug/m^3	3±0 (38.2±1.5)	1±0 (39.8±0)	N/A (0 SD)
Mean $PM_{2.5}$ concentration (μg/m^3)	8.4±6.3	10.0±6.6	0.007
Median $PM_{2.5}$ concentration (μg/m^3)	6.5 (4.3–10.6)	7.8 (5.1–13.4)	0.007
Ambient pollutants months 0–3			
Days with $PM_{2.5}$ higher than 35ug/m^3	10±1.0 (58.1±11.8)	0±0	P<0.0001
Mean $PM_{2.5}$ concentration (μg/m^3)	14.6±16.3	9.1±3.7	P<0.0001
Median $PM_{2.5}$ concentration (μg/m^3)	9.5 (6.0–15.6)	8.8 (6.4–11.4)	P<0.0001
Hours over California 1-h ozone standard	13±2.9	0±0	P<0.0001
Mean ozone level (ppm)	0.032±0.020	0.029±0.017	P<0.001
Median ozone level (ppm)	0.030 (0.016–0.045)	0.027 (0.016–0.040)	P<0.001
Cumulative exposures through sampling date			
Days with $PM_{2.5}$ higher than 35ug/m^3	40±0	29±0.4	P<0.0001
Mean $PM_{2.5}$ concentration (μg/m^3)	9.3±8.0	9.1±7.7	P<0.0001
Median $PM_{2.5}$ concentration (μg/m^3)	8.4 (5.5–13.4)	8.6 (6.3–11.4)	P<0.0001
Hours over California 1-h ozone standard	24±0	7±0	N/A (0 SD)
Mean ozone level (ppm)	0.026±0.015	0.026±0.015	P<0.001
Median ozone level (ppm)	0.025 (0.015–0.036)	0.025 (0.015–0.036)	P<0.001

Note: Age, weight and exposures are shown as mean ± (SD) or median (interquartile range), and compared using t test. Categorical variables (genetic background and corral diversity) are reported as group-specific numerical frequency and compared using Fisher's exact tests. 35ug/m^3 is the 24-hour $PM_{2.5}$ National Ambient Air Quality Standard. 0.09ppm is the California 1-h ozone standard. For the "Days with $PM_{2.5}$ higher than 35ug/m^3" rows, the mean ± SD of the exposure levels in μg/m^3 for those days are shown in parentheses.

Table 2

Methylation status of top ten predicted TF binding sites in public ChIP-seq datasets

Motif	unmethylated	partially methylated	methylated
Fra1/FOSL1	0.68	0.32	0.00
Atf3	0.82	0.18	0.01
JunB	0.88	0.12	0.00
BATF	0.69	0.28	0.03
Fra2/FOSL2	0.90	0.10	0.00
AP-1/Jun	0.81	0.19	0.00
p63/TP53	0.46	0.35	0.19
NF1-halfsite(CTF)/NFIA	0.64	0.31	0.05